



The EUMETSAT
Network of
Satellite
Application
Facilities



NWC SAF VS/AS Scientist Report
Activity period 2016.05.30-2016.09.30

Version: 1.2

Date: 2016.10.27

Feasibility study on retrieval of aerosol mask and optical depth

Final report of NWC SAF Visiting/Associated Scientist Activity

Proposal ref: NWC/CDOP2/SAF/SMHI/SCI/VSP/03

Author:

Jan Paweł Musiał

Institute of Geodesy and Cartography

version 1.2



The EUMETSAT
Network of
Satellite
Application
Facilities



Contents

1	Introduction	5
2	Aim of the study	5
3	Specified tasks	5
4	Input data	5
5	Methodology	6
5.1	LUV method	6
5.2	LUV method improvements	8
5.3	Spectral feature selection	8
5.4	Pre-processing of input data for the AMOR training against the MYD04 AOD product	9
5.5	AMOR development and AOD retrieval	9
6	Results	11
6.1	Prototyping with the CALIOP/MODIS collocation database	11
6.2	Prototyping with the MODIS MYD04 aerosol product	11
6.3	AMOR AOD product inter-comparison	12
6.4	AMOR AOD product validation	13
7	Conclusions	13
8	Outlook	14
	Appendices	15
A	AMOR software description	15

List of Figures

1	Example of a step function to digitize continuous data (reflectance) to integer values.	6
2	AMOR retrieval scheme.	7
3	AMOR prototype based on the PATMOX-x AOD product over ocean. Presented comparison statistics were computed from 400 NOAA18, METOP-A scenes randomly distributed through the year 2008.	8
4	Frequency of the dust occurrence in 2003 derived from the suspended dust flag included in the 28 bit of the MYD35 cloud mask product.	10
5	AMOR AOD retrieval over water based on the CALIOP aerosol/MODIS collocation database.	12
6	AMOR software command line options displayed in a terminal.	15
7	AMOR AOD retrieval prototype for the PPS MODIS processing chain over ocean. The optimized feature selection includes: MODIS band 1 (645 nm), MODIS band 2 (858 nm), MODIS band 7 (2130 nm), satellite zenith angle.	17
8	AMOR AOD retrieval prototype for the PPS VIIRS processing chain over ocean. The optimized feature selection includes: scattering angle, MODIS band 6 (1640 nm), MODIS band 1 (645 nm), satellite zenith angle, MODIS band 2 (858 nm)	17



The EUMETSAT
Network of
Satellite
Application
Facilities



9	AMOR AOD retrieval prototype for the PPS MODIS processing chain over land. The optimized feature selection includes: MODIS band 10 (488 nm), estimated difference at MODIS band 8 (421 nm), estimated difference at MODIS band 1 (645 nm), USGS land cover, and estimated difference at MODIS band 10 (488 nm). For the computation of estimated difference see Section 5.4	18
10	AMOR AOD retrieval prototype for the PPS VIIRS processing chain over land. The optimized feature selection includes: MODIS band 6 (1640 nm), MODIS band 1 (645 nm), USGS land cover.	18
11	Average annual AOD composite from MYD04 product in 2003 retrieved by Deep Blue algorithm.	19
12	Average annual AOD composite from MYD04 product in 2003 retrieved by the fusion of Ocean, Dark Target and Deep Blue algorithms.	19
13	Average annual AOD composite in 2003 retrieved by the AMOR algorithm from the MODIS 11b product.	20
14	Average annual AOD composite in 2003 retrieved by the AMOR algorithm from the MODIS 11b product using the 645 and 1620 nm channels only.	20
15	Frequency of occurrence of the AOD above 0.3 level in 2003 retrieved by the AMOR algorithm from the MODIS 11b product.	21
16	Frequency of occurrence of AOD above 0.3 level in 2003 retrieved by the AMOR algorithm from the MODIS 11b product using the 645 and 1620 nm channels.	21
17	Average annual AOD composite in 2003 retrieved from the MISR data. Credits NASA.	22
18	Average annual AOD composite in 2003 retrieved from the SeaWiFS data. Credits NASA.	22
19	Average annual AOD composite in 2003 retrieved from the OMI data. Credits NASA.	23
20	Validation of the Deep Blue AOD retrievals for the year 2004 against the AERONET measurements.	23
21	Validation of the AMOR AOD retrievals for the year 2004 suited for the PPS MODIS processing chain against the AERONET measurements.	24
22	Validation of the AMOR AOD retrievals for the year 2004 suited for the PPS VIIRS processing chain against the AERONET measurements.	24
23	Comparison of the Deep Blue and AMOR AOD retrievals for the PPS MODIS processing chain for the year 2004 across the selected AERONET sites.	25
24	Comparison of the Deep Blue and AMOR AOD retrievals for the PPS VIIRS processing chain for the year 2004 across the selected AERONET sites.	25



The EUMETSAT
Network of
Satellite
Application
Facilities



NWC SAF VS/AS Scientist Report
Activity period 2016.05.30-2016.09.30

Version: 1.2

Date: 2016.10.27

Acronyms and abbreviations

AERONET - Aerosol Robotic Network
AMOR - Aerosol Mask and Optical depth Retrieval
AOD - Aerosol Optical Depth
AS - Associated Scientist
AVHRR - Advanced Very High Resolution Radiometer
CALIOP - Cloud-Aerosol Lidar with Orthogonal Polarization
CALIPSO - Cloud-Aerosol Lidar and Infrared Pathfinder Satellite Observation
EUMETSAT - European Organisation for the Exploitation of Meteorological Satellites
IGiK - Institute of Geodesy and Cartography
IR - Infra Red
LUV - Look-Up Vector
LUT - Look-Up Table
MetImage-Meteorological Imager
MODIS - Moderate Resolution Imaging Spectroradiometer
MOD04 - MODIS Aerosol product TERRA platform
MOD35 - MODIS Cloud Mask Product TERRA platform
MSG - Meteosat Second Generation
MTG - Meteosat Third Generation
MYD02 - MODIS L1B product AQUA platform
MYD04 - MODIS Aerosol product AQUA platform
MYD10 - MODIS Snow Mask product AQUA platform
MYD35 - MODIS Cloud Mask product AQUA platform
NCEP - National Centers for Environmental Prediction
NWC SAF - Satellite Application Facility on Support to Nowcasting & Very Short Range Forecasting
NWP - Numerical Weather Prediction
Suomi NPP - Suomi National Polar-orbiting Partnership satellite
PATMOS-x - AVHRR Pathfinder Atmospheres - Extended
PCM - Probabilistic Cloud Mask
PPS - Polar Platform System
SMHI - Swedish Meteorological and Hydrological Institute
SWIR - Short Wave Infra Red
VFM - Vertical Feature Mask
VIRR - Visible and Infra-Red Radiometer
VIIRS - Visible/Infrared Imager and Radiometer Suite
VS- Visiting Scientist



The EUMETSAT
Network of
Satellite
Application
Facilities



NWC SAF VS/AS Scientist Report
Activity period 2016.05.30-2016.09.30

Version: 1.2

Date: 2016.10.27

1 Introduction

Information about atmospheric aerosols is of great importance for all domains of optical remote sensing including satellite meteorology and climatology. For this reason improvements of the aerosol flag dataset derived by the EUMETSAT NWC SAF PPS version v2017/2018 software are to be implemented. In this scope, the EUMETSAT NWC SAF issued a feasibility study under the framework of Visiting Scientist (VS)/Associated Scientist (AS) activity. The study was organised into two 14 days VS activities at the beginning and at the end of the Project separated by 2 months of the AS activity. Time frame of the activity spanned from 30.05.2016 to 30.09.2016.

2 Aim of the study

The primary objective of the presented study was to develop the AMOR (Aerosol Mask and Optical depth Retrieval) prototype algorithm based on MODIS imagery and evaluate its performance by means of the AERONET measurements. The AMOR concept was based on the LUV (Look-Up Vector) technique proposed by Musial et al. (2014b) and improved in Musial et al. (2014a). The secondary objective of the study was to verify the portability of the method to other satellite sensors (i.e. VIIRS onboard Suomi NPP satellite).

3 Specified tasks

Within the study the following tasks were defined:

1. To develop the AMOR algorithm based on the heritage PCM method using MODIS imagery selected for aerosol prototyping in PPS.
2. To evaluate the performance and investigate spectral channel selection within the AMOR algorithm.
3. To investigate the discrimination of heavy aerosol loads complemented by the AOD retrieval by means of the AMOR method applied to MODIS data.
4. To compile the VS/AS report including a detailed description of the method and prototyping results. The report should also recommend the next development steps in case of promising prototyping results, elaborate on possible applicability of the methodology to MSG/MTG sensors and in the appendix technically describe software developed in the frame of VS/AS.

4 Input data

The first phase of the AMOR prototyping was based on the MODIS/CALIOP collocation database compiled by the SMHI within the WP 4713C. The database consisted of the CALIOP aerosol product at 5 km resolution (oversampled to 1 km) and the AQUA MODIS MYD02 L1B product at 1 km resolution. The prototyping results were not satisfactory due to small number of collocations that hindered the AMOR training under a wide range of atmospheric and angular conditions. Therefore, the reference data sets used for the AMOR training were changed to:

- AQUA MODIS MYD04 aerosol product at 10 km resolution
- MYD02 L1B product resampled to 10 km

- MYD35 cloud mask at 1 km resolution
- MYD10 snow mask at 0.5 km resolution

The reference AOD data sets used for the AMOR AOD training were based on the two MYD04 collection 6 data sets: "Optical_Depth_Land_And_Ocean" and "Deep_Blue_Aerosol_Optical_Depth_550_Land". The first dataset (Figure 12) contains AOD estimates derived by fusion of the 3 algorithms: "Ocean algorithm", "Deep blue" and "Dark Target". This data was used to train AMOR over ocean because of stringent quality screening over land which treats all reflective surfaces (e.g. deserts) as unreliable. Therefore, over land the AMOR algorithm was trained against the "Deep_Blue_Aerosol_Optical_Depth_550_Land" dataset that includes reflective surfaces (Figure 11).

To assess the AMOR AOD retrieval accuracy global in-situ AOD measurements from the AERONET network for the year 2004 were used.

5 Methodology

This section describes the LUV method and its adaptation to the AOD retrieval within the AMOR algorithm.

5.1 LUV method

The Look-Up Vector (LUV) approach proposed by Musial et al. (2014a) is an extension of the Probabilistic Cloud Mask (PCM) algorithm (Musial et al., 2014b). Its concept is based on a multidimensional sparse matrix, called the information space, which dimensions are composed of discrete features such as: spectral channels, satellite/Sun angular data and ancillary information (e.g. NWP fields). In order to transform continuous data (e.g. spectral channels) to a discrete form the set of step functions is employed (Figure 1). Further, all of the discrete datasets are combined into a single feature of a vector form by means of bitwise operations i.e. bit position shift and bitwise OR. As a result each unique combination of the information space features is described by a single value, which serves as a LUV index. During the algorithm training process, for each index value a statistical estimate of a desired quantity (e.g. mean AOD or its standard deviation) is computed from the accumulated training data. This leads to derivation of separate LUVs for each quantity of interest including separate LUV indexes.

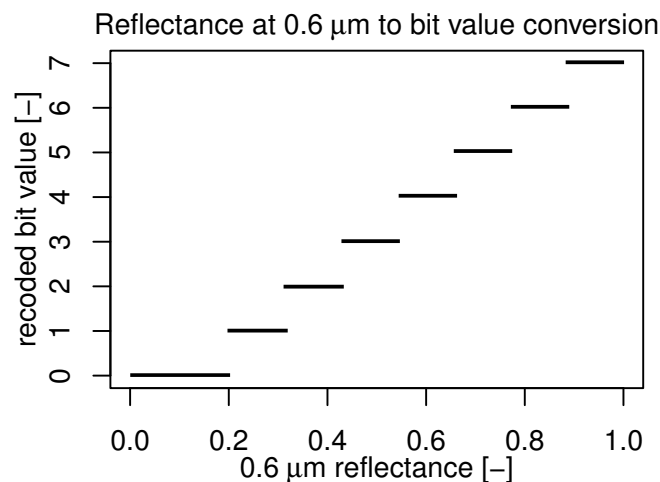


Figure 1: Example of a step function to digitize continuous data (reflectance) to integer values.

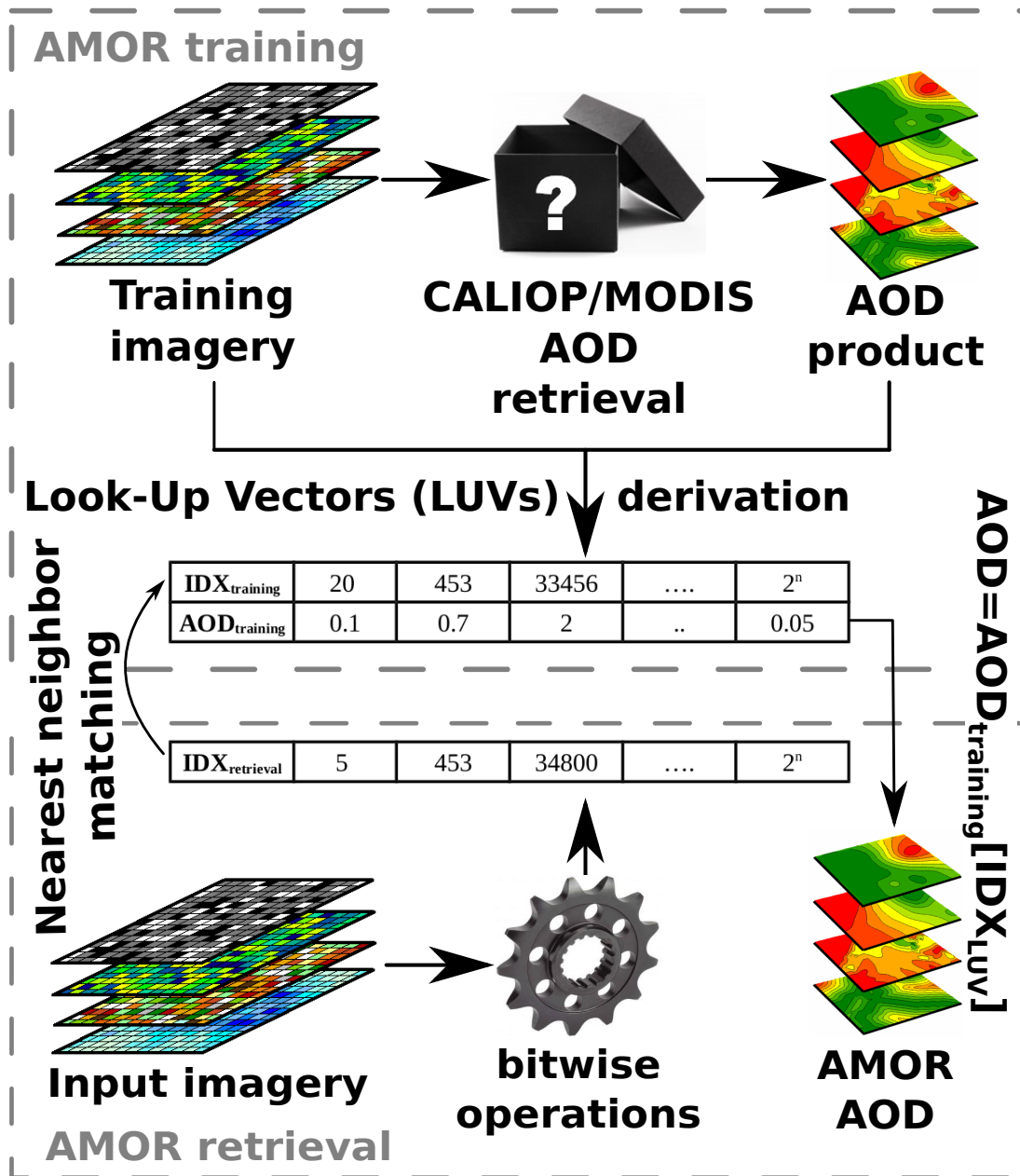


Figure 2: AMOR retrieval scheme.

The satellite product retrieval is limited to the derivation of the LUV indexes by means of the step functions and the bitwise operators (Figure 2). Further the derived LUV index is located by means of the nearest neighbour technique within the LUV indexes acquired during the algorithm training. The retrieved positions of each pixel from input imagery within the training LUV allows for the extraction of desired quantity estimates. Such an approach eliminates complicated on-the-fly computations e.g. employing radiative transfer models, because all of the numerically demanding processing can be performed once during the algorithm training and stored within the LUV. This significantly improves the processing time and accurately approximates the original retrieval (Figure 3).

5.2 LUV method improvements

Initially the parametrization of the LUV technique, such as feature selection and scaling of the step functions, was set arbitrary using expert knowledge. Recently, this has been improved by implementing an interactive procedure that involves the algorithm training and evaluation at each step. The purpose of this operation is to maximise the correlation coefficient (in case of the continuous data e.g AOD) or the Cohen's kappa coefficient (in case of the discrete data e.g. cloud phase classification) computed between retrievals and the reference data. This optimization is performed in two steps, where initially the most suitable feature sequence is derived from a set of features using a first guess of scaling factors step functions. In the next step, the scaling factors are optimized using the most optimal feature sequence retrieved in the previous step. Consequently, the parametrization of the LUV method is derived in an objective way that maximizes the retrieval accuracy.

5.3 Spectral feature selection

The initial selection of the bands (421, 488, 645, 858, 2130 nm) followed closely the MYD04 MODIS aerosol product (Levy et al., 2013; Kaufman et al., 1997) to verify the nominal accuracy of the AMOR algorithm. Further, a subset of the spectral channels (645, 858, 1640 nm) was selected to ensure a basic AVHRR channel heritage and transferability of the AMOR AOD retrieval to other sensors such as: AVHRR, METIMAGE, VIRR, VIIRS, MSG, and MERSI-2. For the more a number of these sensors, dedicated algorithms could be developed that take advantage of more aerosol sensitive channels. Deterioration of the retrieval accuracy between the MODIS channel setup and the basic AVHRR heritage channel setup was assessed by validation against the AERONET AOD measurements.

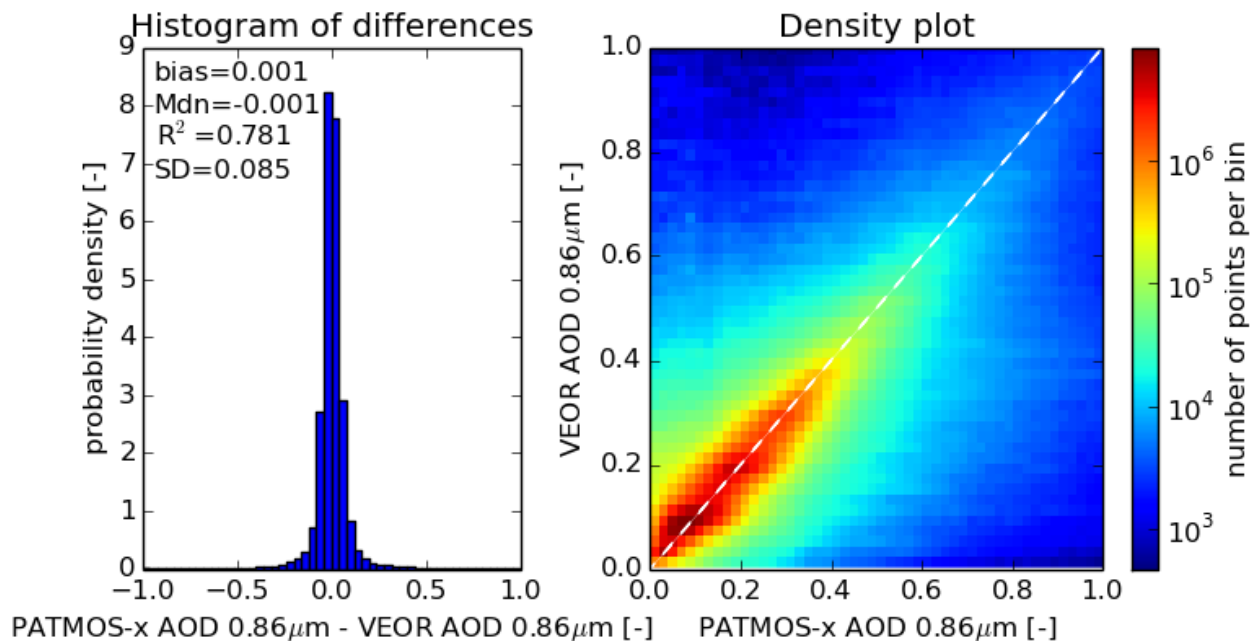


Figure 3: AMOR prototype based on the PATMOX-x AOD product over ocean. Presented comparison statistics were computed from 400 NOAA18, METOP-A scenes randomly distributed through the year 2008.



5.4 Pre-processing of input data for the AMOR training against the MYD04 AOD product

Development of the AMOR algorithm was based on the training database composed of randomly selected samples from MODIS imagery from the year 2003 and the analogous reference database from the year 2004. At the beginning, prototyping was performed using the data sets embedded in the MYD04 AOD product at 10 km resolution including the atmospherically and BRDF corrected reflectances. Nevertheless, to assure the compatibility with the PPS software which uses uncorrected reflectance there was a need to compile a new MODIS reflectance dataset in the same way as for the MOD04 product. Consequently, influence of the atmospheric and BRDF effects on the reflectance is already included within the AMOR LUVs, that reduces computational demand during retrieval. Derivation of the new reflectance dataset followed closely the methodology described by Levy et al. (2013) involving the following steps:

1. Resampling of the MYD10 0.5 km product to 1 km.
2. Masking of cloud, snow cover and inland water bodies from the MYD02 11b 1km product using the MYD35 and MYD10 level 2 products.
3. Screening pixels below and above the certain percentiles of reflectance within the 10x10 pixel/km window to remove remaining cloudiness and cloud shadows.
 - 3.1. Over land all pixels below 25% and above 50% percentile were screened using the 2130 nm reflectance.
 - 3.2. Over ocean all pixels below 25% and above 75% percentile were screened using the 860 nm reflectance.
4. Reduce resolution of the screened and masked MODIS spectral bands to 10x10 km by averaging the data within the 10x10 pixel windows.

Once the new reflectance dataset had been generated, it was further used to compute a Look-Up Table (LUT) that stores the MODIS reflectance at: band 8 (421 nm), band 10 (488 nm), band 1 (645 nm), band 6 (1640 nm), and band 7 (2130 nm); as a function of the Normalize Difference Vegetation Index (NDVI), the satellite zenith angle, and the scattering angle. Unlike approach proposed by Levy et al. (2013), where the database contained the lowest envelope of reflectance at a certain scattering angle, the AMOR solution involves computation of reflectance at the 0.3 AOD level reported by the MYD04 product. Nevertheless, both approaches share the same concept of relating the observed reflectance to a reference value retrieved within the aerosol-free atmosphere or within the aerosol-loaded atmosphere with a certain concentration. During the AMOR prototyping such data sets were introduced to improve the retrieval accuracy. They were computed as a difference between the observed reflectance and the one retrieved from the LUT.

5.5 AMOR development and AOD retrieval

Prerequisite for the AMOR prototyping was to develop fast yet accurate algorithm that would supplement the PPS cloud mask product with the flag delineating regions of high aerosol loads. Common approach to this task involves thresholding of brightness temperature differences between the IR channels (Ackerman, 1997). Further, selection of the VIS/NIR channels may be included (Ackerman et al., 2010) to improve the retrieval during daytime. Example of such a product is depicted on Figure 4, where it is clearly visible that only some of the regions (Sahara and Taklimakan deserts) of high aerosol loads are distinguished as opposed to the MYD04 AOD product (Figure 12). For this reason it was decided to first retrieve AOD by means of the AMOR method and then to apply the threshold of 0.3 AOD to discriminate between aerosol-free and aerosol-loaded atmosphere.

The AMOR training was performed for two spectral features setups (see Section 5.3) in order to be applicable to the PPS MODIS processing chain and to the AVHRR heritage chain that extracts only 3 reflective bands

Dust fraction in 2003 from MODIS MYD35 cloud mask

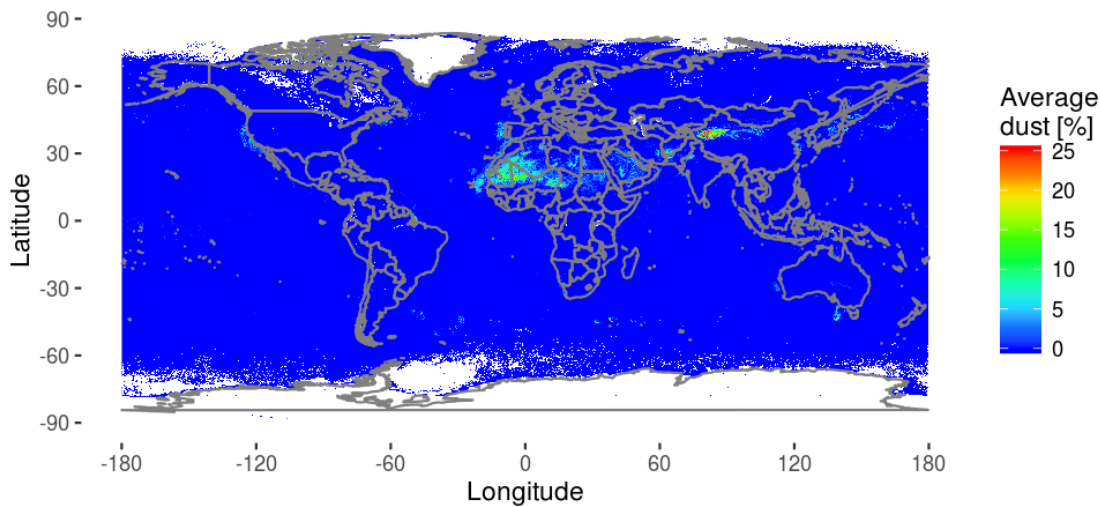


Figure 4: Frequency of the dust occurrence in 2003 derived from the suspended dust flag included in the 28 bit of the MYD35 cloud mask product.

(645, 858, 1640 nm) out of all available bands. Since the AVHRR heritage chain was tested on VIIRS data, it is referred to as PPS VIIRS in this report. The first phase of this process comprised of optimization of the feature selection and the step functions scaling factors. This iterative procedure at each step involved: the AMOR training against samples from the year 2003, retrieving AOD estimates for the year 2004 and computing correlation coefficient with the MYD04 AOD product from the year 2004. Separate optimizations were performed over land and ocean to fit the Ocean and the Deep Blue AOD retrieval algorithms. The most optimal parametrization deeming the highest correlation coefficient was further employed to train the AMOR against all the available data from the year 2003 (and not only the random samples). The LUVs derived during the algorithm training are stored within a single HDF5 file composed of two dataset groups dedicated to the MODIS and VIIRS sensors. Within each group data sets are divided between land and ocean and they comprise of the following information: mean estimates, standard deviation and AOD value counts for every LUV index (which describes unique feature combination). Furthermore, the HDF5 groups have attributes that describe the features and scaling factors combinations together with a number of bits that each feature occupies.

The AMOR retrieval begins with extracting attributes for the HDF5 group dedicated to a particular satellite sensor. Consequently, the information about the features and scaling factors combinations together with the number of bits allows for computation of the index values by means of the step functions and the bitwise operations. Further, these values are located within the LUV indexes stored within the HDF5 groups using the nearest neighbour technique. Then for each LUV position the mean estimates of AOD, its standard deviation and value counts are extracted. Ultimately, the following AMOR products are generated:

- AOD estimates
- standard deviation of the AOD estimates that indicates retrieval quality
- number of values used to compute the AOD estimates
- aerosol flag that delineates regions with the AOD greater than 0.3



The EUMETSAT
Network of
Satellite
Application
Facilities



6 Results

The presented analysis was performed to evaluate quality of the AMOR AOD retrieval using the CALIOP/MODIS collocation database and the MODIS MYD04 aerosol product as a reference data. It consisted of inter-comparison between the AMOR retrieval and reference data, validation against the AERONET measurements, and visual comparison of level 3 AOD product maps. Most of the analysis was based on the MODIS data acquired in the year 2004 (not used for the AMOR training) apart from the level 3 product analysis that for the sake of smoothness required large data volume downloaded for the year 2003 (and used for the AMOR training).

6.1 Prototyping with the CALIOP/MODIS collocation database

The CALIPSO and AQUA platforms follow each other closely within the A-train satellite constellation. Consequently the CALIOP sensor onboard CALIPSO platform and the MODIS instrument onboard AQUA platform are collocated globally at nadir view within the ~ 73 second time difference. This allows for complex cloud physical properties studies using a passive radiometer and an active LIDAR system. In this respect SMHI derived the CALIOP/AQUA MODIS database composed of global collocations acquired during 24 days from the year 2010 (2 days per month). The nominal resolution of the CALIOP Aerosol product is 5 km which within the database was oversampled to 1 km in order to match the MODIS MYD02 11b product. The aerosol product consisted of a number of Scientific Data Sets amongst which the following were present: column AOD estimates, cloud fraction and Sun zenith angle. They were used to discriminate clear-sky daytime AOD estimates defined as pixels with a cloud fraction equal zero and Sun zenith angle lower than 84° . After this screening around 200 000 samples were left, which were further divided into training (~ 190 000 samples) and test (~ 10 000 samples) data sets. The best run of the AMOR prototyping with the CALIOP/MODIS matchup data base over ocean resulted in the AOD correlation of 0.391 and the standard deviation of 0.193 (Figure 5). It was concluded that the number of samples is not sufficient to cover different environmental conditions encountered in the test data set. As a result the nearest neighbour matching of the LUV indexes within the AMOR algorithm lead to incorrect selection of the AOD estimates. Another source of uncertainties comes from the oversampling of the 5 km CALIOP aerosol Product to 1 km. This leads to the situation where 5 consecutive pixels from the MODIS sensor featuring different spectral signatures are described by the single CALIOP AOD estimate.

6.2 Prototyping with the MODIS MYD04 aerosol product

The unsatisfactory prototyping results acquired using the CALIOP/MODIS collocation database lead to a change of the reference data to the 10 km MODIS MYD04 aerosol product (Levy et al., 2013). It contains the AOD estimates generated by the 3 retrieval algorithms: the Ocean algorithm (Tanré et al., 1997), enhanced Deep Blue algorithm over land (Hsu et al., 2013), and the Dark Target algorithm over land (Levy et al., 2009). To obtain full spatial cover the first two algorithms were used as the last one does not provide AOD estimates over reflective surfaces.

Concerning the AMOR AOD retrieval over ocean it agrees very well ($R^2 > 0.92$) with the reference MYD04 AOD "Ocean algorithm". Slightly better results were obtained using the prototype suited for the PPS MODIS processing chain (Figure 7) due to availability of the reflectance at 2130 nm. The AMOR prototype suited for the PPS VIIRS processing chain (Figure 8) exploits the scattering angle together with the subset of the VIIRS bands at 645, 858, 1640 nm (to ensure the portability to older sensors e.g. AVHRR as explained in Section 5.5).

Prototyping results over land are of lesser quality as compared to the ocean cases due to a complex nature and dynamics of a surface reflectance. Especially influence of the AOD on reflectance over the bright targets is limited therefore bands in blue spectra are required to obtain higher sensitivity. This is clearly visible while comparing the AMOR AOD prototypes for the PPS MODIS and PPS VIIRS processing chains (Figures 9 & 10).

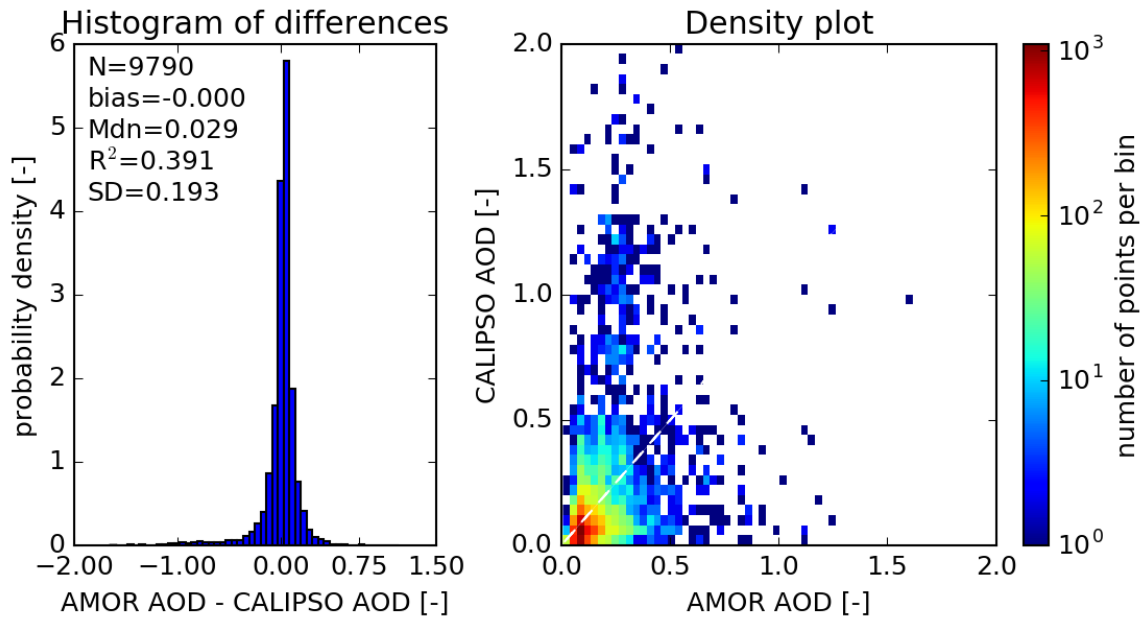


Figure 5: AMOR AOD retrieval over water based on the CALIOP aerosol/MODIS collocation database.

The first one utilizes the full range of MODIS channels whereas the second is limited to the 3 channel subset of VIIRS bands excluding the reflectances in blue spectra. Consequently the correlation coefficient decreases from 0.73 to 0.52. Influence of the surface reflectance on the AOD is also highlighted by the fact that the USGS land cover was selected during the AMOR optimization for the the MODIS and VIIRS processing chains. The overall accuracy of the AMOR retrievals as compared to the reference MYD04 AOD product is moderate. Nevertheless, it is sufficient to delineate regions above the 0.3 AOD threshold that was used to generate the AMOR Aerosol Mask (AMA) product.

6.3 AMOR AOD product inter-comparison

The MYD04, AMOR AOD, and AMA level 2 products were combined to 0.1 x 0.1 degree mean annual composites for the year 2003. This allows for the analysis of spatial patterns and for a comparison with other satellite AOD products available on the "<http://disc.sci.gsfc.nasa.gov/giovanni>".

Over ocean the AMOR AOD prototypes for the MODIS and VIIRS processing chains (Figures 13 & 14) are quite consistent with the reference MYD04 data (Figure 12) as well as with the SeaWiFS and MISR AOD products (Figures 18 & 17). The most apparent difference is with the OMI AOD product (Figure 19) that reports significantly higher values. Nevertheless, all of the products exhibit similar spatial pattern with high AOD values over the West coast of Africa, southern part of the Red Sea, and eastern part of the Arabian Sea. It is related to the transport of the desert dust and it is well visible in the case of the AMOR AMA products (Figures 15 & 16).

Over land consistency of the AOD products is substantially lower even between the MYD04 products (Figures 12 & 11). This is also visible while comparing the AMOR AOD prototypes for the PPS MODIS and VIIRS processing chains (Figures 13 & 14), where due to unavailability of bands in the deep blue spectra, the latter product reports lower AOD values. On average sensitivity of the AMOR AOD retrievals is lower than the reference MYD04 Deep Blue AOD retrievals (Figure 11). Nevertheless, the spatial patterns are preserved what is reflected in the AMOR AMA products (Figures 15 & 16). Other products reports lower AOD values than the Deep blue algorithm (Figure 11) especially over Eastern Siberia. This region was affected by severe, durable



forest fires that caused vast smoke plumes. The MYD04 and AMOR products (Figures 12 & 11 & 13 & 14) were able to capture this phenomena while the SeaWiFS and OMI AOD data sets (Figures 18 & 19) revealed insensitivity to the smoke.

6.4 AMOR AOD product validation

The validation of AMOR and MYD04 AOD retrievals was performed against the global AERONET measurements from the year 2004 (Figures 20 & 21 & 22). Overall agreement with the AERONET across all of the products is at similar, moderate level ($R^2 \sim 0.64$). However, the best linear fit is achieved by the MYD04 Deep Blue product and the worst one with the AMOR prototype for the PPS VIIRS processing chain (due to lack of channels in the blue spectra). The validation analysis revealed very similar AOD retrieval accuracy between the MYD04 Deep blue algorithms and the AMOR prototype for the PPS MODIS processing chain. Nevertheless, it has to be emphasized that the AERONET stations are mostly located over vegetated areas that feature low reflectance at the 645 nm band. This increases sensitivity to aerosol concentration and facilitates the AOD retrieval. Consequently, agreement between the MYD04 and AMOR AOD products presented for the selected AERONET sites (Figures 23 & 24) is better than the one reported for the global data (Figures 9 & 10).

7 Conclusions

The main conclusion of this feasibility study is that the LUV method (Musial et al., 2014a) implemented in the AMOR prototype algorithm is suitable for the AOD retrieval and for the aerosol flag discrimination. The inter-comparison and validations analyses performed against the reference MYD04 AOD product as well as other independent sources confirmed the spatial consistency and accuracy of the AMOR retrieval. The specific conclusions of this study are listed below:

- The CALIOP/MODIS collocation database does not have sufficient number of samples for the AMOR prototyping. Furthermore, oversampling of the 5 km CALIOP Aerosol product to the 1 km MODIS 11b grid introduces uncertainties related to mapping of several MODIS pixels to a single AOD estimate.
- The MODIS Aerosol product (MYD04/MOD04) is suitable for the AMOR prototyping and features moderate AOD retrieval accuracy as compared to the AERONET measurements.
- Over ocean the "Optical_Depth_Land_And_Ocean" MYD04 dataset can be used for the AMOR prototyping whereas over land the "Deep_Blue_Aerosol_Optical_Depth_550_Land" dataset should be used. The reason for this is that the "Dark Target" AOD retrieval algorithm (embedded in the former MYD04 product) does not provide estimates over bright surfaces (such as deserts) as opposed to the "Deep Blue" method.
- The AMOR algorithm has to include separate LUVs at least for the land and ocean retrievals as the AMOR optimization varies across different land covers.
- The reflectance at 2.11 μm is more suitable for the AOD retrieval than the reflectance at 1.63 μm which is apparent while comparing the AOD products over ocean generated by the AMOR prototypes suited for the PPS MODIS and VIIRS processing chains.
- The AMOR AOD retrieval over ocean features almost perfect agreement with the reference MYD04 product.
- The AMOR AOD retrieval over land varies significantly between the prototypes suited for the PPS MODIS and VIIRS processing chains revealing good to moderate agreement with the reference MYD04 product.



The EUMETSAT
Network of
Satellite
Application
Facilities



NWC SAF VS/AS Scientist Report
Activity period 2016.05.30-2016.09.30

Version: 1.2

Date: 2016.10.27

"Deep Blue" dataset. This is caused by unavailability of bands in the blue spectra within the VIIRS processing chains that significantly deteriorates sensitivity of the method to aerosol concentration.

- The threshold of 0.3 AOD accurately delineates regions of high aerosol loads and as such was selected for the AMOR Aerosol MAsk (AMA) product.
- All of the AMOR products reveal similar spatial patterns as the reference MYD04 products reporting lower values (~ 0.2 lower) at the same time.
- The AMOR and MYD04 AOD products reveal greater sensitivity to smoke over Eastern Siberia than the AOD products generated from other satellite sensors (MISR, SeaWiFS, and OMI).
- Due to reduces spectral resolution, the AMOR prototype suited for the PPS VIIRS processing chain is applicable to a wide range of polar orbiting satellite instruments including: METIMAGE, VIRR and AVHRR. In case of the geostationary instruments such as MSG more extensive study is required to asses the influence of different viewing geometry on the AOD retrievals.

8 Outlook

Satisfactory results of this feasibility study should encourage further development of the AMOR prototype and its implementation within the NWC SAF PPS processing chain. The next development steps should involve:

1. Expansion of the temporal coverage of input MODIS data to the entire years 2003 and 2004.
2. Further development of the reference reflectance database based on a larger number of data sets.
3. Derivation of separate LUVs for different land cover types.
4. Feasibility study on aerosol type discrimination by means of the LUV approach using the MODIS TERRA and MISR AOD products.
5. Application of the AMOR algorithm to geostationary satellite data.

Appendices

A AMOR software description

The AMOR algorithm suited for the PPS data processing was implemented in the Python programming language as a single script executable from the command line. The AMOR command line options together with the descriptions are presented on Figure 6. The required satellite input data consists of: PPS satellite MODIS/VIIRS file, Sun/satellite acquisition geometry file, PPS physiography file and PPS cloud mask file. Other required inputs are: AMOR LUV file and LUT reflectance database. Optional input parameters are predefined, however they can be altered by a user (output directory, AOD threshold for AMA products, and buffer around clouds in pixels to exclude from retrieval). The software is suited for the Linux computers with the following dependencies installed: Python \geq 2.6, hdf5 library with Python h5py package, Python numpy package.

```
jane@maluch:~$ ~/Dropbox/scripts/python/python2.7/src/smhi/PGE_AMOR_v4.py -h
Usage: PGE_AMOR_v4.py [options]

Options:
  --version                show program's version number and exit
  -h, --help              show this help message and exit
  -a FILE_ANGLES, --pps-angles-file=FILE_ANGLES
                        REQUIRED: Full path to PPS sunsatangles file matching
                        pattern: S_NWC_sunsatangles_*.h5
  -b BSIZE, --cloud-buffer-size=BSIZE
                        OPTIONAL: Buffer size in pixels around clouds to
                        exclude from analysis. Default=5
  -c FILE_CMA, --pps-cma-file=FILE_CMA
                        REQUIRED: Full path to PPS cloud mask file matching
                        pattern: S_NWC_CMA_*.h5
  -l FILE_LUV_AOD, --luv-file=FILE_LUV_AOD
                        REQUIRED: Full path to AMOR LUV file.
  -o OUTDIR, --output-dir=OUTDIR
                        OPTIONAL: Path to output directory. Default is the
                        directory of the S_NWC_CMA_*.h5 file.
  -p FILE_LC, --pps-physiography-file=FILE_LC
                        REQUIRED: Full path to PPS physiography matching
                        pattern: S_NWC_physiography_*.h5
  -r FILE_LUV_REFLECTANCE, --reflectance-luv=FILE_LUV_REFLECTANCE
                        REQUIRED: Full path to AMOR reflectance LUV file.
  -s FILE_SAT, --pps-satellite-file=FILE_SAT
                        REQUIRED: Full path to PPS satellite matching pattern:
                        S_NWC_[SatSensor]_[SatName]_*.h5
  -t AMA_TRESHOLD, --ama-threshold=AMA_TRESHOLD
                        OPTIONAL: AOD treshold for Aerosol Msk (AMA) product.
```

Figure 6: AMOR software command line options displayed in a terminal.



The EUMETSAT
Network of
Satellite
Application
Facilities



NWC SAF VS/AS Scientist Report
Activity period 2016.05.30-2016.09.30

Version: 1.2

Date: 2016.10.27

References

- Ackerman, S., Frey, R., Strabala, K., Yinghui, L., Gumley, L., Baum, B., and Menzel, W.: Discriminating clear-sky from cloud with modis. Algorithm theoretical basis document (MOD35), Tech. Rep. 6.1, Cooperative Institute for Meteorological Satellite Studies, University of Wisconsin - Madison, 2010.
- Ackerman, S. A.: Remote sensing aerosols using satellite infrared observations, *Journal of Geophysical Research: Atmospheres*, 102, 17 069--17 079, 1997.
- Hsu, N., Jeong, M.-J., Bettenhausen, C., Sayer, A., Hansell, R., Seftor, C., Huang, J., and Tsay, S.-C.: Enhanced Deep Blue aerosol retrieval algorithm: The second generation, *Journal of Geophysical Research: Atmospheres*, 118, 9296--9315, 2013.
- Kaufman, Y., Tanré, D., Remer, L. A., Vermote, E., Chu, A., and Holben, B.: Operational remote sensing of tropospheric aerosol over land from EOS moderate resolution imaging spectroradiometer, *Journal of Geophysical Research: Atmospheres*, 102, 17 051--17 067, 1997.
- Levy, R., Mattoo, S., Munchak, L., Remer, L., Sayer, A., and Hsu, N.: The Collection 6 MODIS aerosol products over land and ocean, *Atmos. Meas. Tech*, 6, 2989--3034, 2013.
- Levy, R. C., Remer, L. A., Tanré, D., Mattoo, S., and Kaufman, Y. J.: Algorithm for remote sensing of tropospheric aerosol over dark targets from MODIS: Collections 005 and 051: Revision 2; Feb 2009, Download from http://modisatmos.gsfc.nasa.gov/_docs/ATBD_MOD04_C005_rev2.pdf, 2009.
- Musial, J., Hüsler, F., Sütterlin, M., Neuhaus, C., and Wunderle, S.: Day-time low stratiform cloud detection on AVHRR imagery, *Remote Sensing*, (in press), 2014a.
- Musial, J., Hüsler, F., Sütterlin, M., Neuhaus, C., and Wunderle, S.: Probabilistic approach to cloud and snow detection on Advanced Very High Resolution Radiometer (AVHRR) imagery, *Atmospheric Measurement Techniques*, 7, 799--822, 2014b.
- Tanré, D., Kaufman, Y., Herman, M., and Mattoo, S.: Remote sensing of aerosol properties over oceans using the MODIS/EOS spectral radiances, *Journal of Geophysical Research: Atmospheres*, 102, 16 971--16 988, 1997.

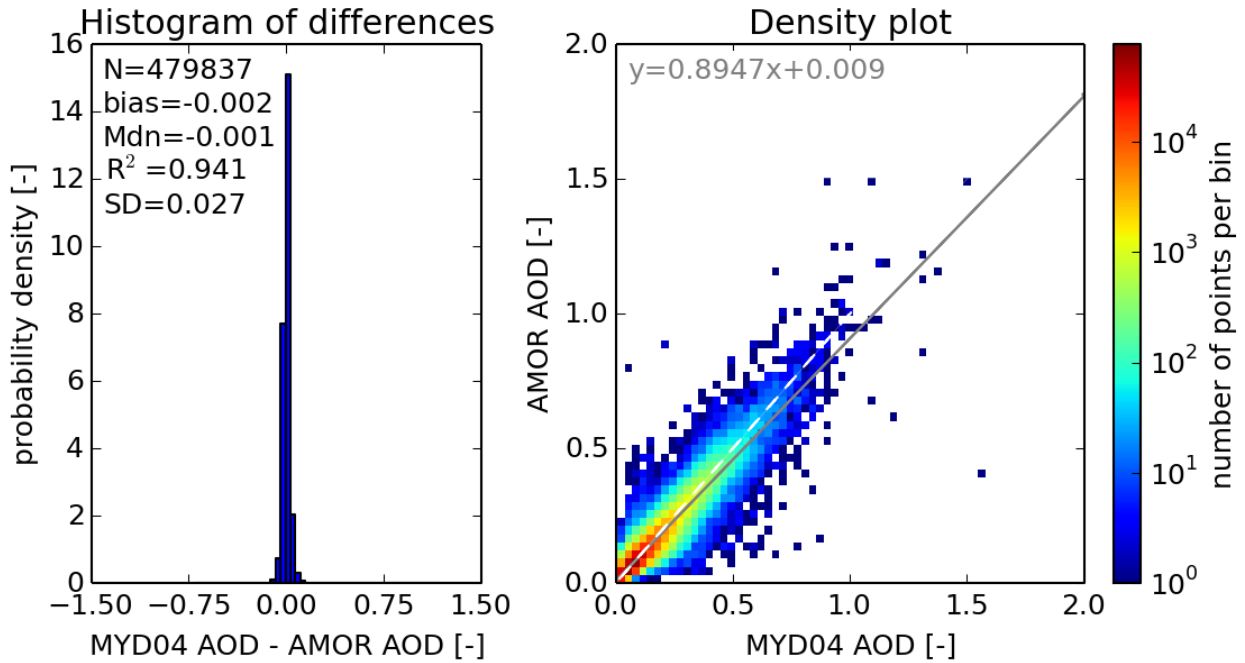


Figure 7: AMOR AOD retrieval prototype for the PPS MODIS processing chain over ocean. The optimized feature selection includes: MODIS band 1 (645 nm), MODIS band 2 (858 nm), MODIS band 7 (2130 nm), satellite zenith angle.

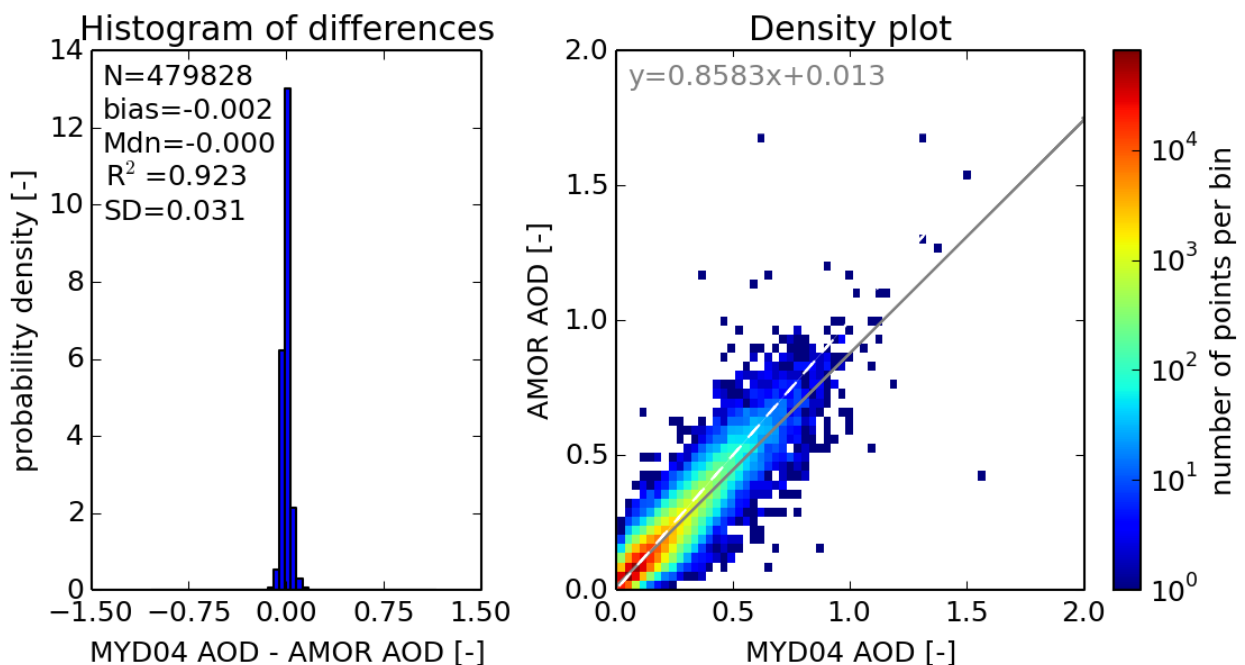


Figure 8: AMOR AOD retrieval prototype for the PPS VIIRS processing chain over ocean. The optimized feature selection includes: scattering angle, MODIS band 6 (1640 nm), MODIS band 1 (645 nm), satellite zenith angle, MODIS band 2 (858 nm)

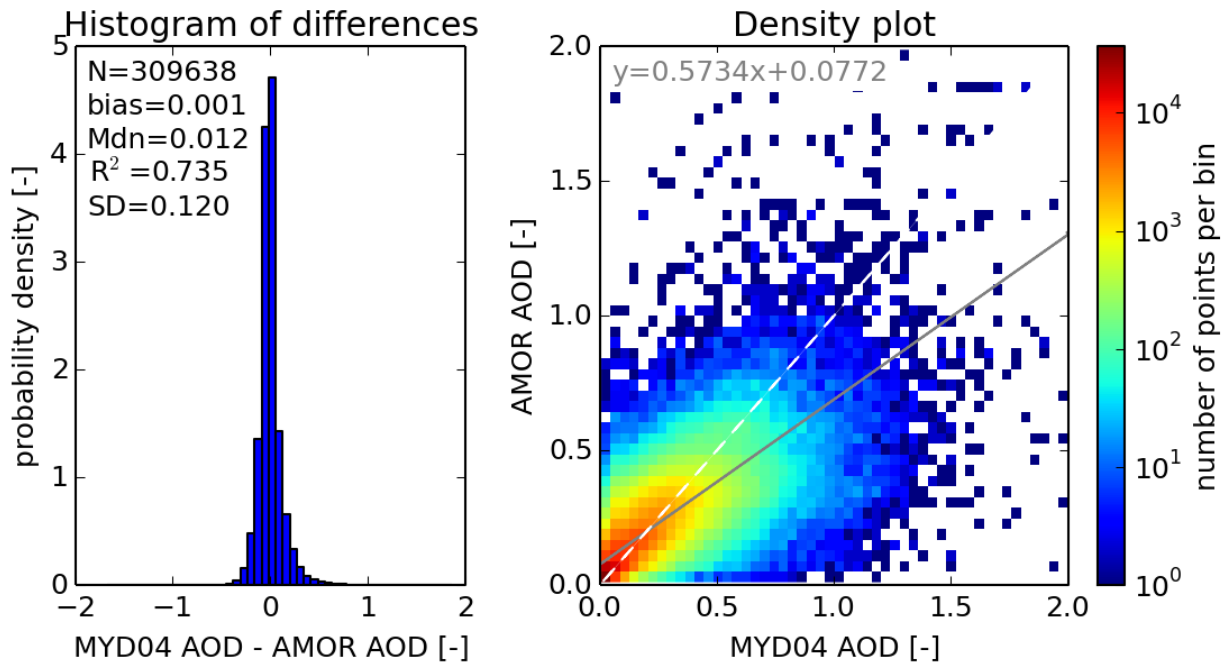


Figure 9: AMOR AOD retrieval prototype for the PPS MODIS processing chain over land. The optimized feature selection includes: MODIS band 10 (488 nm), estimated difference at MODIS band 8 (421 nm), estimated difference at MODIS band 1 (645 nm), USGS land cover, and estimated difference at MODIS band 10 (488 nm). For the computation of estimated difference see Section 5.4

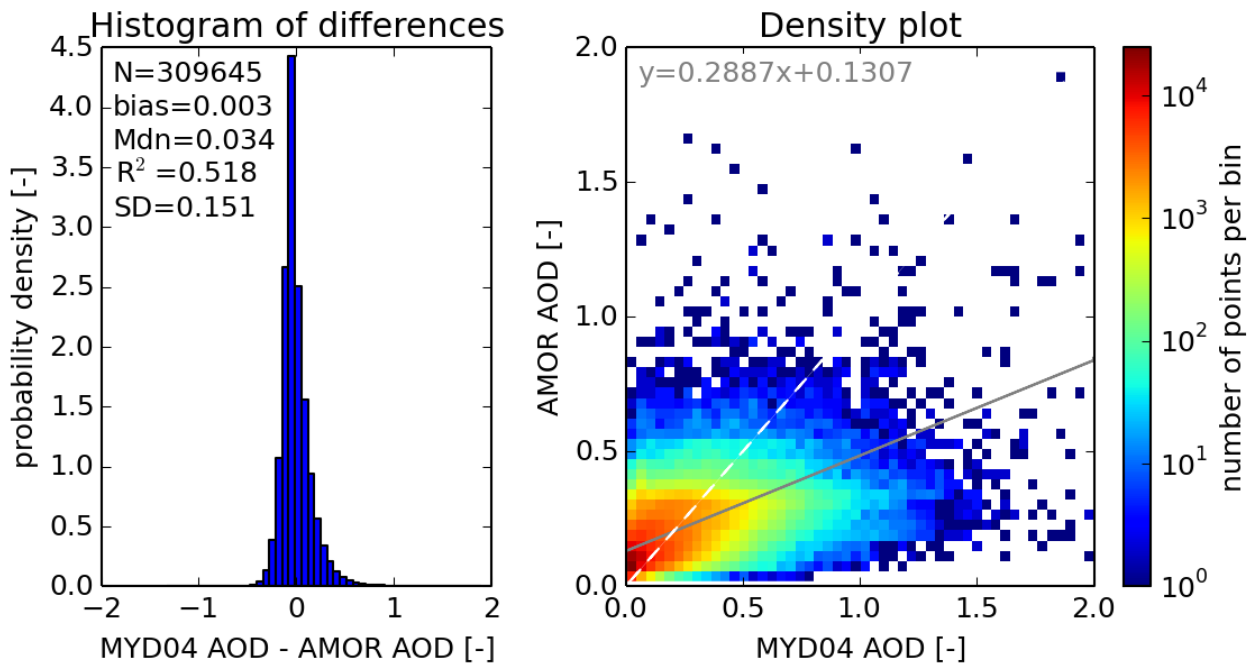


Figure 10: AMOR AOD retrieval prototype for the PPS VIIRS processing chain over land. The optimized feature selection includes: MODIS band 6 (1640 nm), MODIS band 1 (645 nm), USGS land cover.

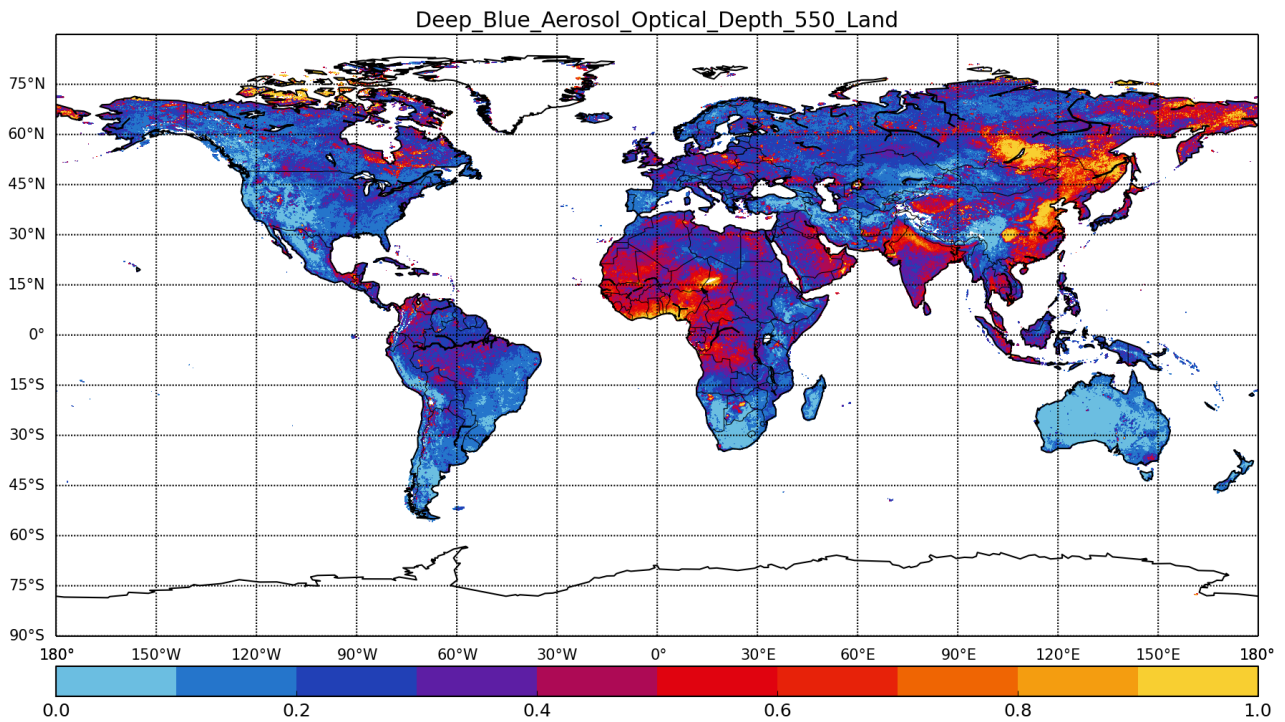


Figure 11: Average annual AOD composite from MYD04 product in 2003 retrieved by Deep Blue algorithm.

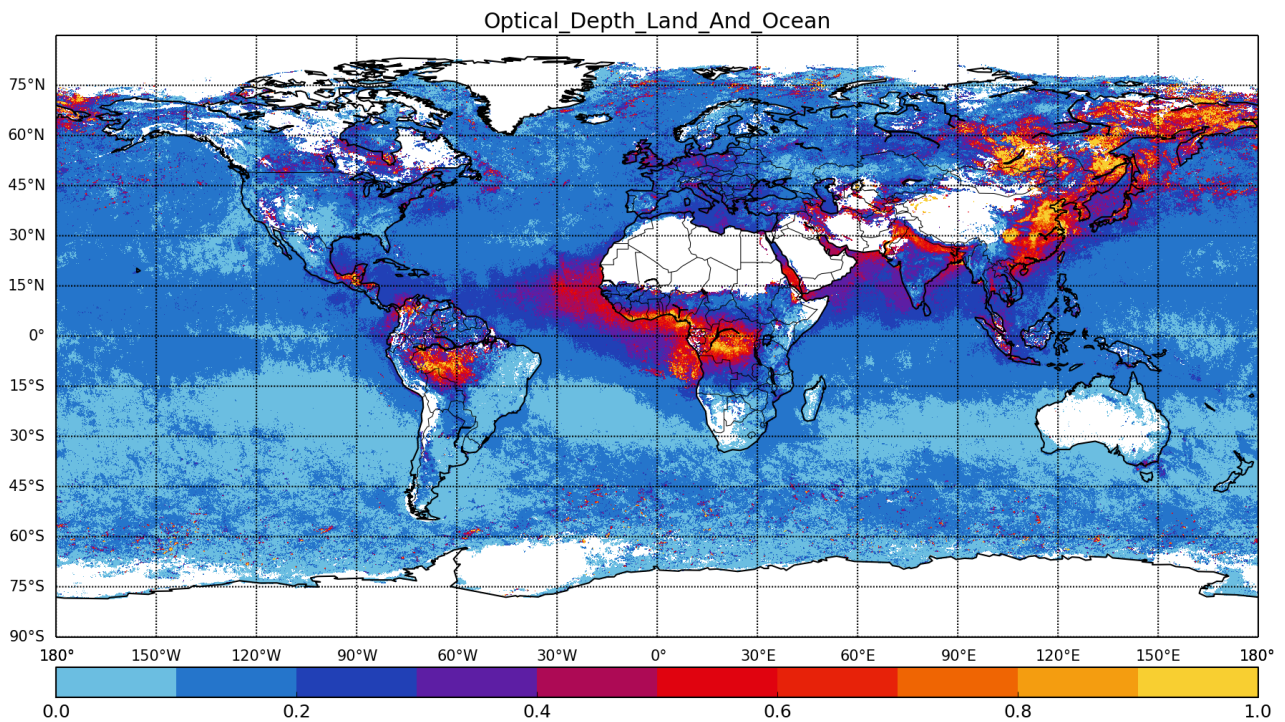


Figure 12: Average annual AOD composite from MYD04 product in 2003 retrieved by the fusion of Ocean, Dark Target and Deep Blue algorithms.

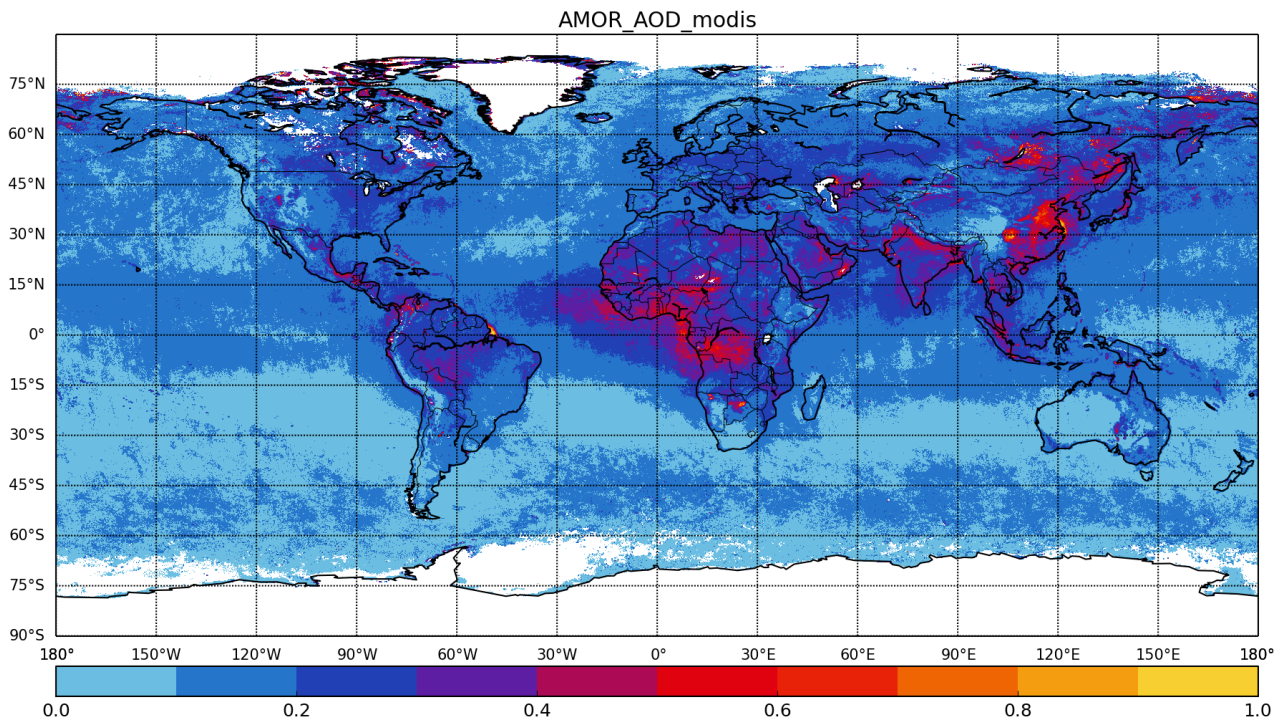


Figure 13: Average annual AOD composite in 2003 retrieved by the AMOR algorithm from the MODIS 11b product.

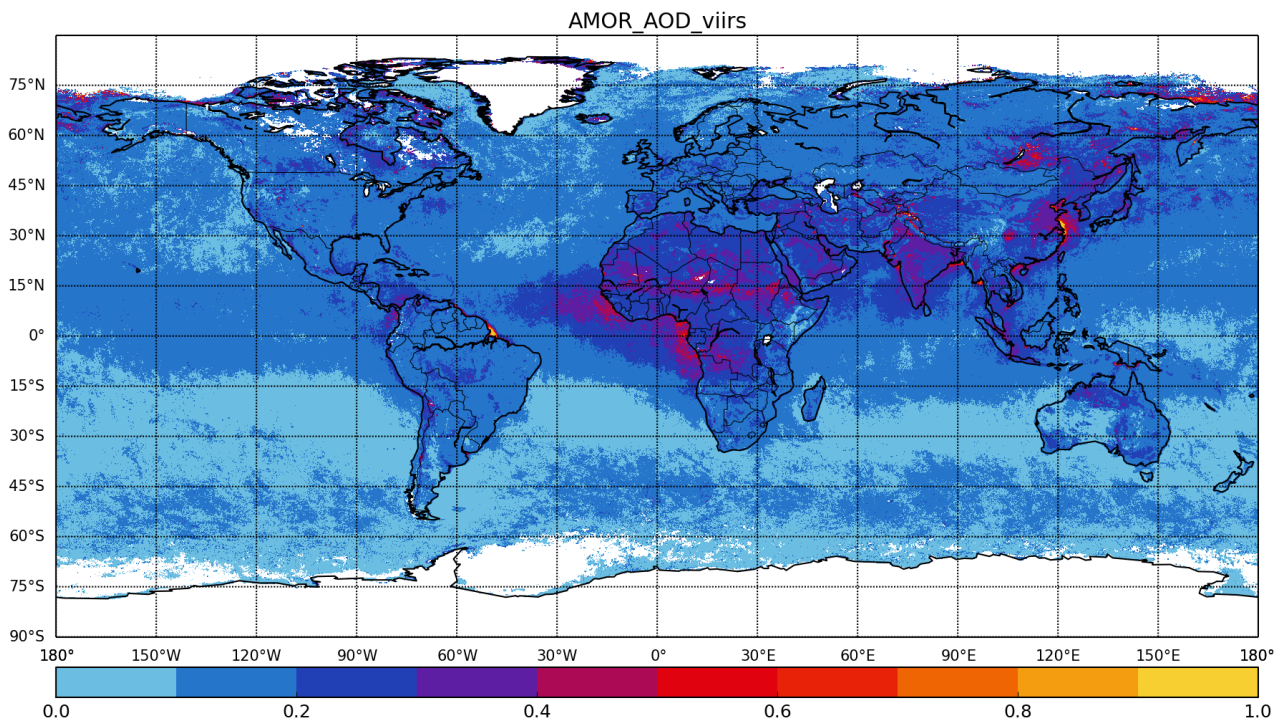


Figure 14: Average annual AOD composite in 2003 retrieved by the AMOR algorithm from the MODIS 11b product using the 645 and 1620 nm channels only.

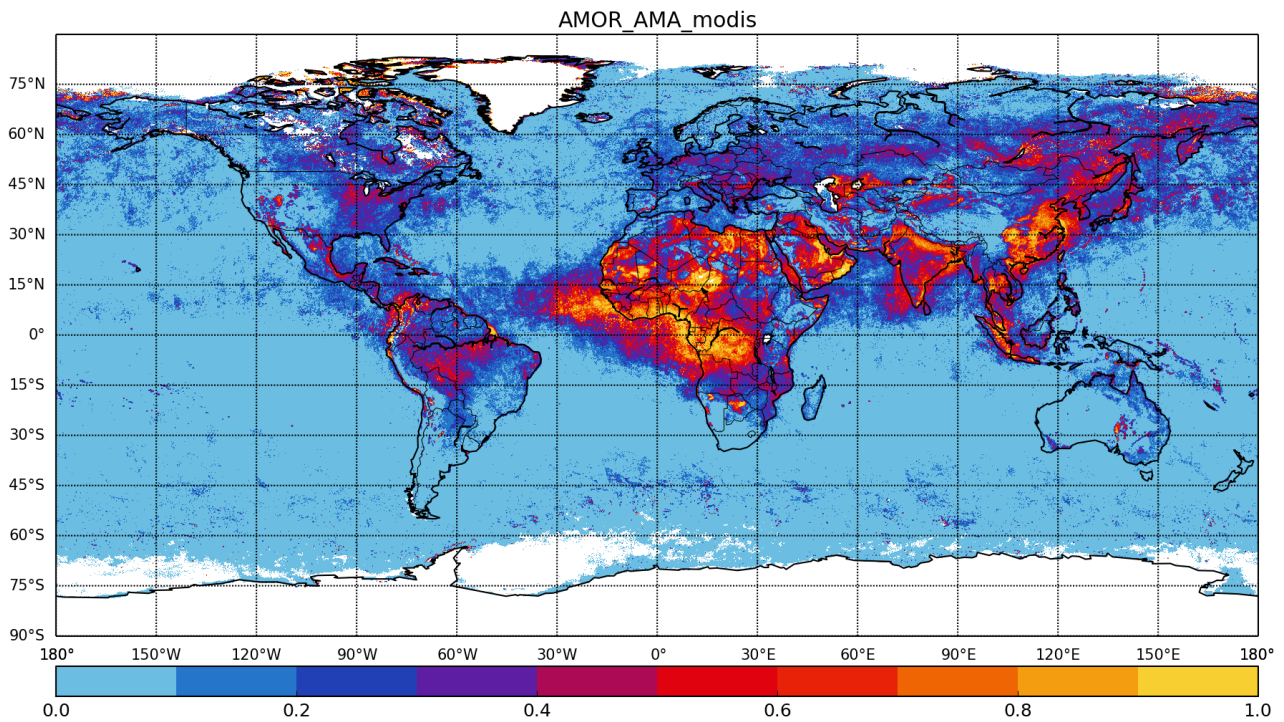


Figure 15: Frequency of occurrence of the AOD above 0.3 level in 2003 retrieved by the AMOR algorithm from the MODIS 11b product.

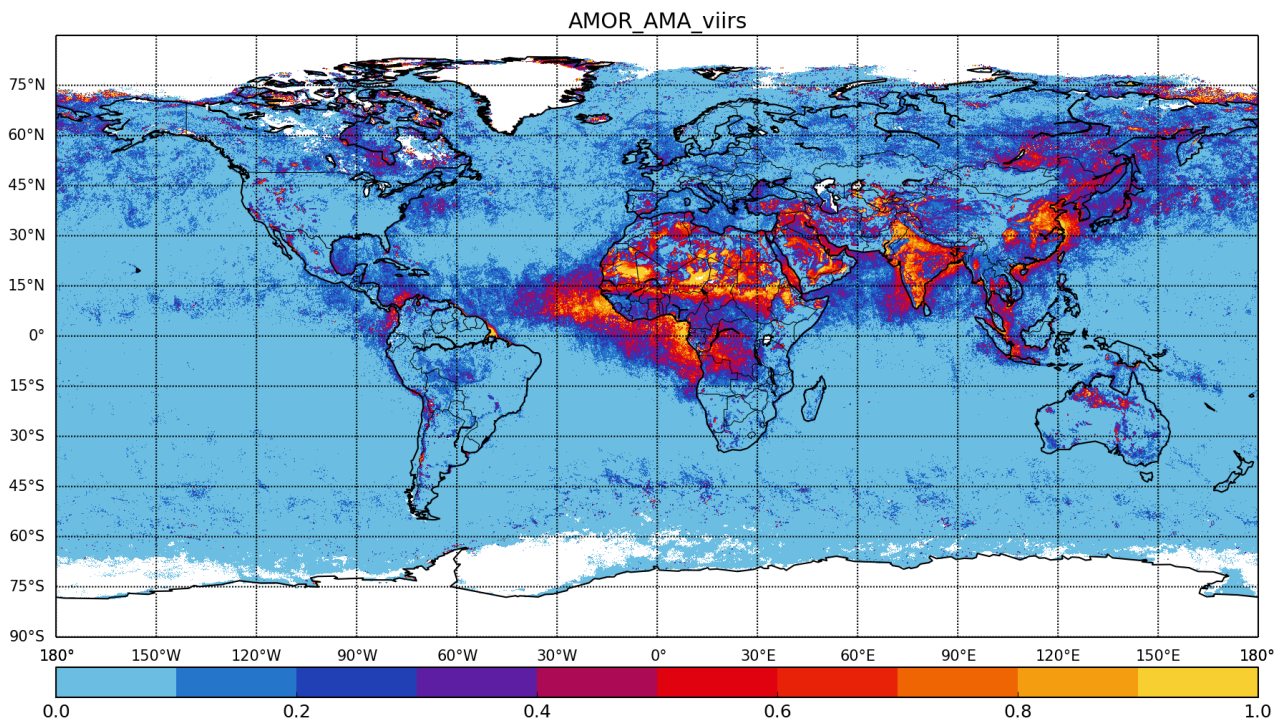
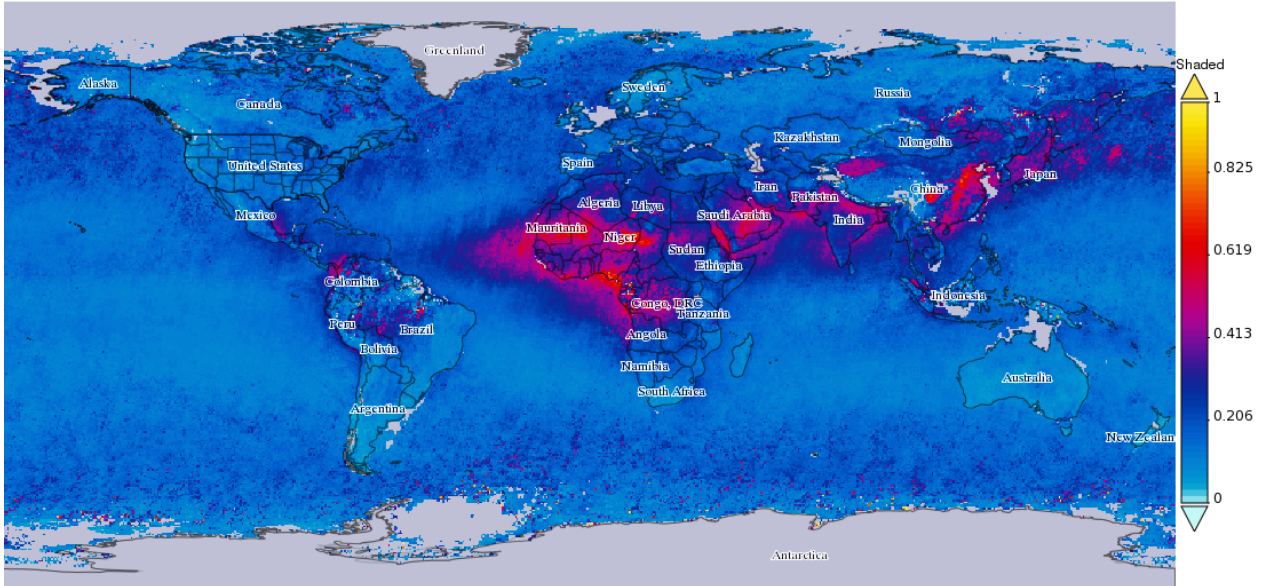


Figure 16: Frequency of occurrence of AOD above 0.3 level in 2003 retrieved by the AMOR algorithm from the MODIS 11b product using the 645 and 1620 nm channels.

Time Averaged Map of Aerosol Optical Depth 555 nm daily 0.5 deg. [MISR MIL3DAE v4]
over 2003-01-02 - 2003-12-31, Region 180W, 90S, 180E, 90N



- Selected date range was 2003-01-01 - 2003-12-31. Title reflects the date range of the granules that went into making this result.

Figure 17: Average annual AOD composite in 2003 retrieved from the MISR data. Credits NASA.

Time Averaged Map of Aerosol Optical Depth 550 nm daily 0.5 deg. [SeaWiFS SWDB_L305 v004]
over 2003-01-01 - 2003-12-31, Region 180W, 90S, 180E, 90N

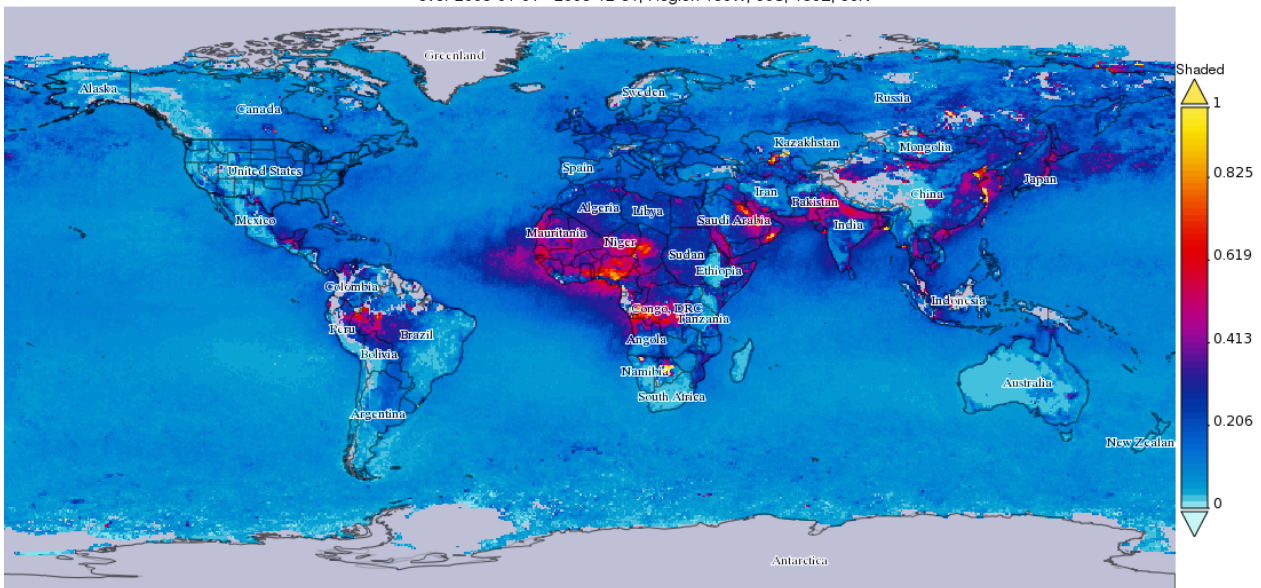


Figure 18: Average annual AOD composite in 2003 retrieved from the SeaWiFS data. Credits NASA.

Time Averaged Map of Aerosol Optical Depth 500 nm daily 1 deg. [OMI OMAERUVd v003]
over 2005-01-01 - 2005-12-31, Region 180W, 90S, 180E, 90N

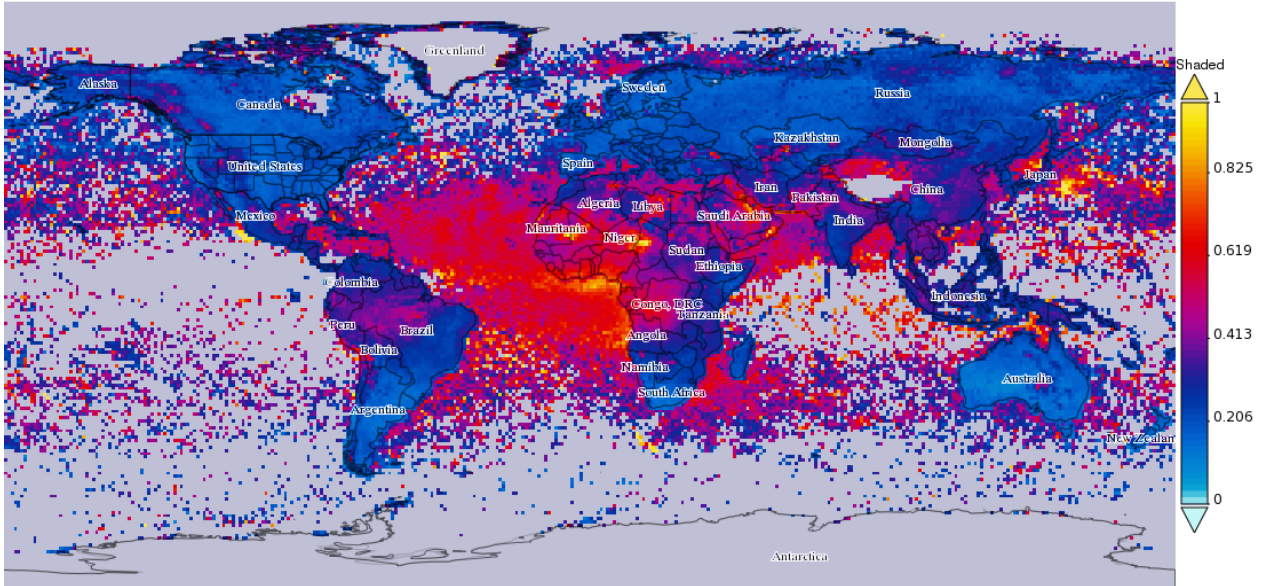


Figure 19: Average annual AOD composite in 2003 retrieved from the OMI data. Credits NASA.

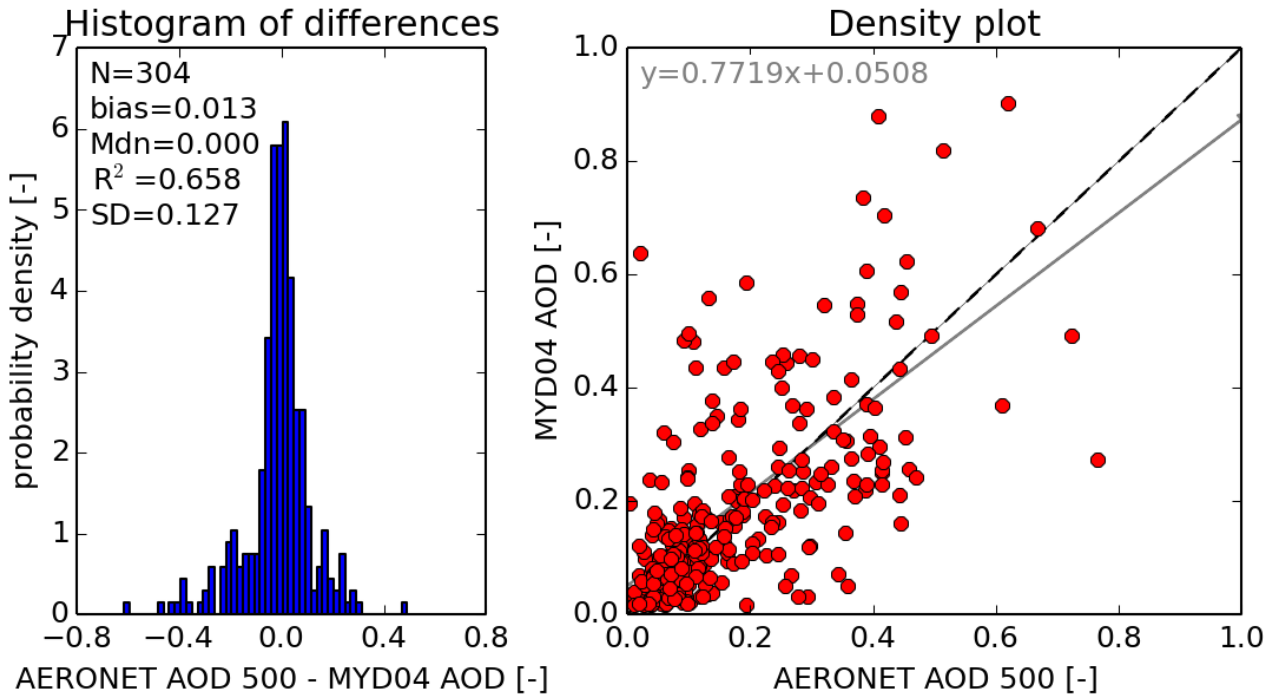


Figure 20: Validation of the Deep Blue AOD retrievals for the year 2004 against the AERONET measurements.

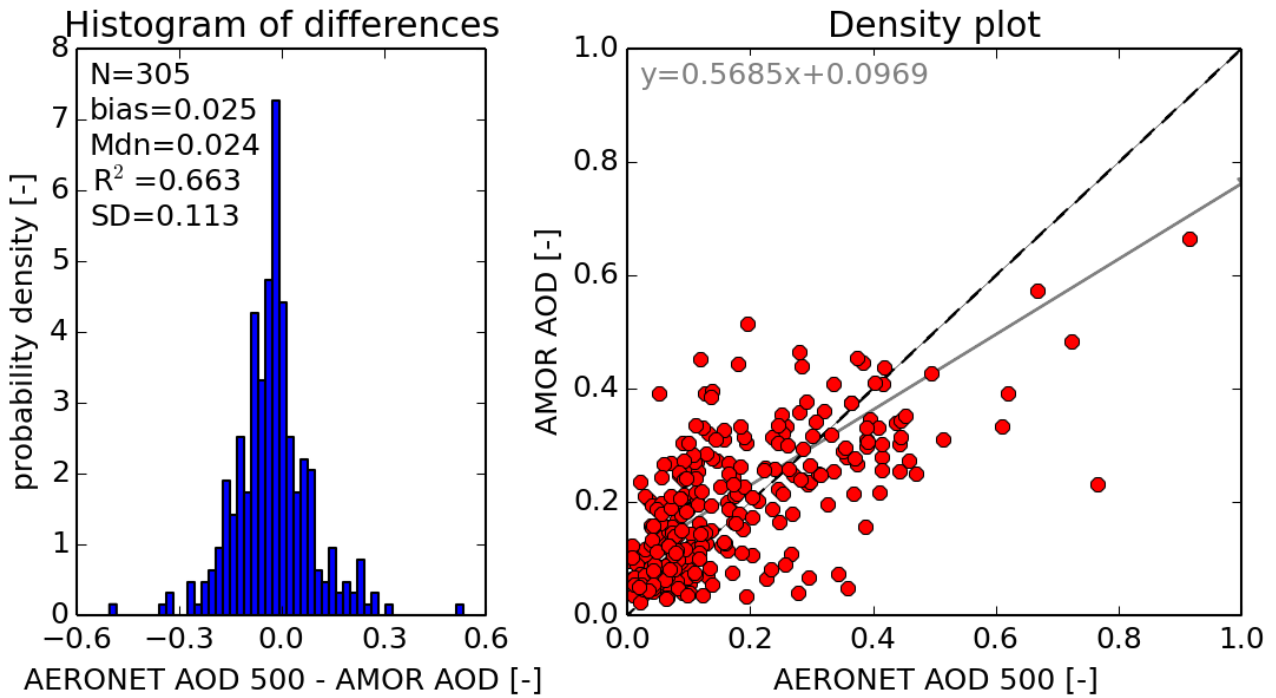


Figure 21: Validation of the AMOR AOD retrievals for the year 2004 suited for the PPS MODIS processing chain against the AERONET measurements.

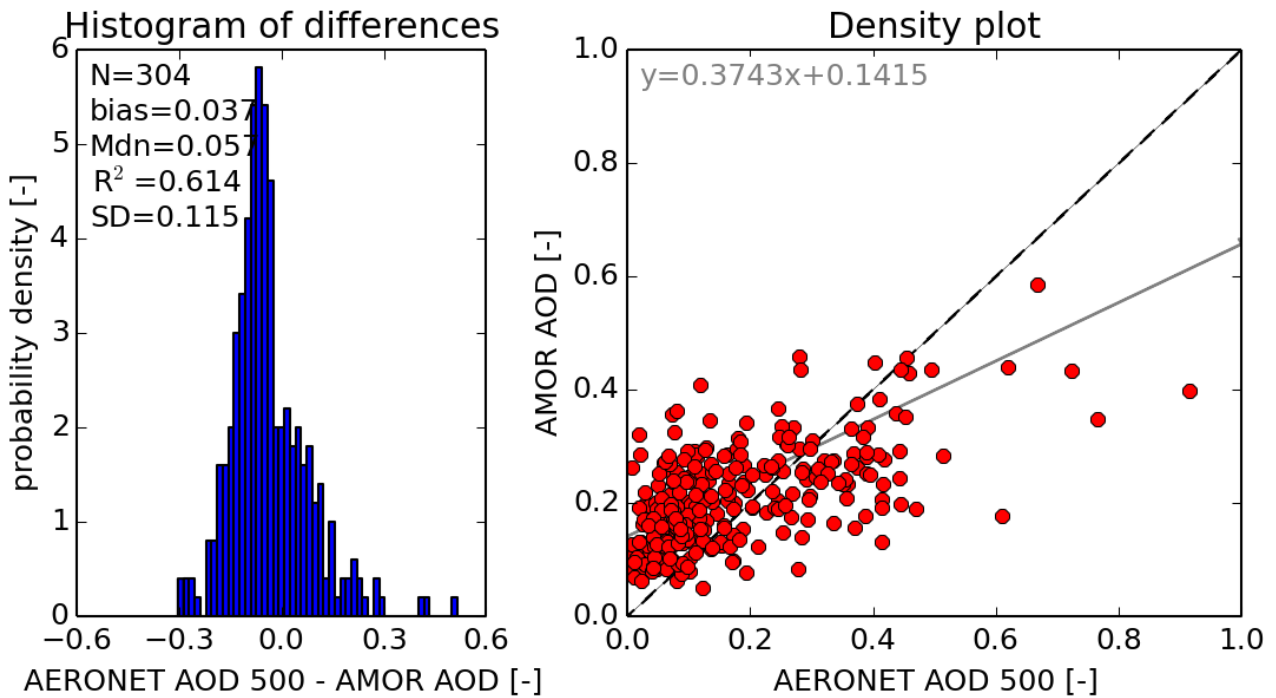


Figure 22: Validation of the AMOR AOD retrievals for the year 2004 suited for the PPS VIIRS processing chain against the AERONET measurements.

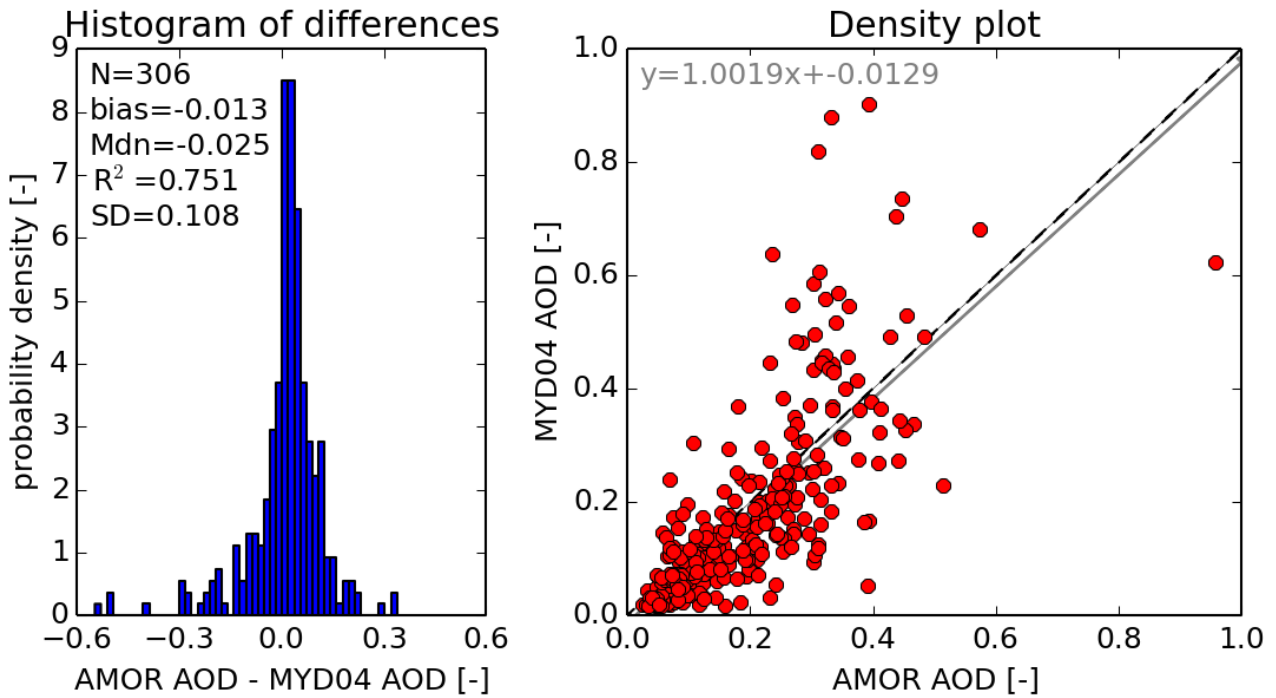


Figure 23: Comparison of the Deep Blue and AMOR AOD retrievals for the PPS MODIS processing chain for the year 2004 across the selected AERONET sites.

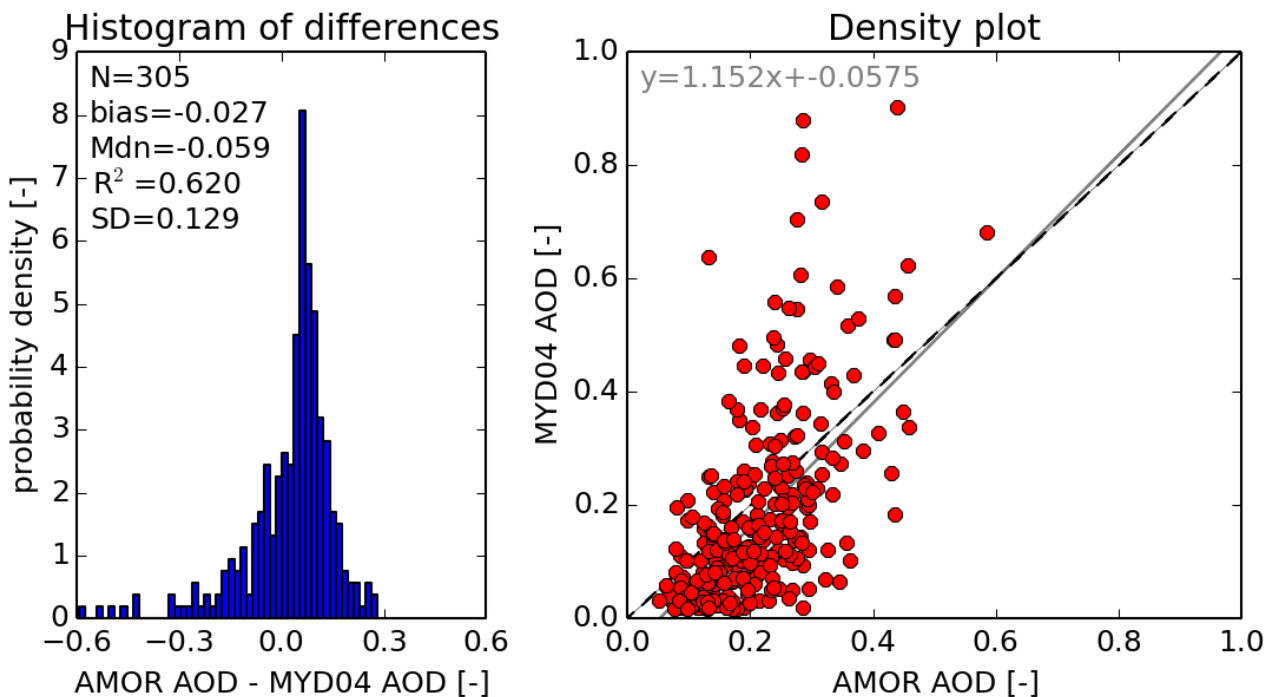


Figure 24: Comparison of the Deep Blue and AMOR AOD retrievals for the PPS VIIRS processing chain for the year 2004 across the selected AERONET sites.